PCCP

Accepted Manuscript

Volume 1 | Number 1 | Jan 2013 | Pages 1–100
PCCP
Physical Chemistry Chemical Physics
www.rsc.org/pccp
ROYAL SOCIETY OF CHEMISTRY

This is an *Accepted Manuscript*, which has been through the Royal Society of Chemistry peer review process and has been accepted for publication.

Accepted Manuscripts are published online shortly after acceptance, before technical editing, formatting and proof reading. Using this free service, authors can make their results available to the community, in citable form, before we publish the edited article. We will replace this *Accepted Manuscript* with the edited and formatted *Advance Article* as soon as it is available.

You can find more information about *Accepted Manuscripts* in the Information for Authors.

Please note that technical editing may introduce minor changes to the text and/or graphics, which may alter content. The journal's standard Terms & Conditions and the Ethical guidelines still apply. In no event shall the Royal Society of Chemistry be held responsible for any errors or omissions in this *Accepted Manuscript* or any consequences arising from the use of any information it contains.

ROYAL SOCIETY OF CHEMISTRY

www.rsc.org/pccp

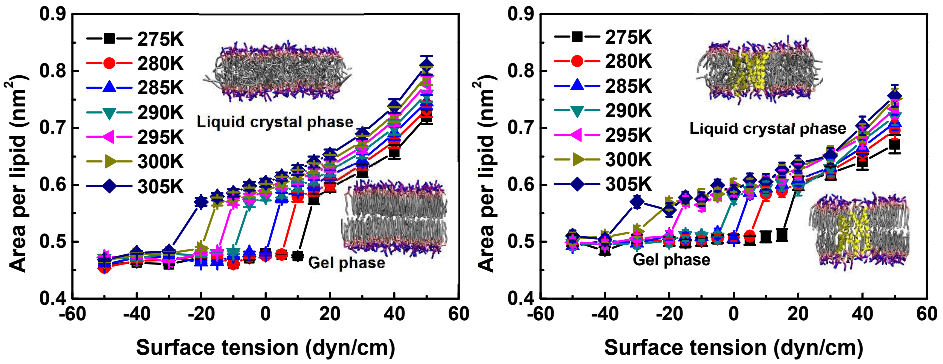
275K
280K
285K
290K
295K
300K
305K
Liquid crystal phase
Gel phase
Area per lipid (nm^2)
Surface tension (dyn/cm)
0.4
0.5
0.6
0.7
0.8
0.9
-60
-40
-20
0
20
40
60

Cite this: DOI: 10.1039/c0xx00000x

www.rsc.org/xxxxxx

PAPER

Surface tension effects on the phase transition of a DPPC bilayer with and without protein: A molecular dynamics simulation†

Xian Kong[a], Shanshan Qin[b], Diannan Lu[*a], Zheng Liu[*a]

Received (in XXX, XXX) Xth XXXXXXXXX 20XX, Accepted Xth XXXXXXXXX 20XX

DOI: 10.1039/b000000x

While the surface tension of a cell membrane, or plasma membrane, regulates cell functions, little is known about its effect on the conformational changes of the lipid bilayer and hence the resulting changes to the cell membrane. To obtain some insight into the phase transition of the lipid bilayer as a function of surface tension, we used a 1,2-dipalmitoyl-*sn*-glycero-3-phosphocholine (DPPC) bilayer as a model lipid bilayer and aquaporin (AqpZ), a transmembrane channel protein for water, as a model embedded protein. A coarse-grained molecular dynamics simulation was applied to illustrate the phase transition behavior of the pure DPPC bilayer and aquaporin-embedded DPPC bilayer under different surface tensions. It was shown that an increased surface tension reduced the phase transition temperature of the DPPC bilayer. As for the DPPC bilayer in gel form, no significant changes occurred to the structure of the bilayer in response to the surface tension. Once in a liquid crystal state, both the structure and properties of the DPPC bilayer, such as area per lipid, lipid order parameter, bilayer thickness and lateral diffusion coefficients, were responsive to the magnitude of surface tension in a linear way. The presence of aquaporin attenuated the compact alignment of the lipid bilayer, hindered the parallel movement, and thus made the DPPC bilayer less sensitive to the surface tension.

Introduction

In vivo, the surface tension of plasma membranes of cells regulates the biological, physical and chemical functions of the cell[1], such as endocytosis, exocytosis, cell motility, cell spreading, photoresponsiveness[2] and mechanoresponsiveness.[3] *In vitro* lipid vesicles embedded with membrane proteins in bio-sensors[4] and bio-separation[5] devices may also experience the changes in the environmental osmolality, which leads to changes of surface tension[6] of bilayers in a much larger scale than in biological environment and thus affects the performance of these devices.

Phase transitions are basic and important phenomena for lipid bilayer and could influence its structural and dynamical properties greatly. There are many factors controlling phase transitions, like temperature, lipid components, and tail length of lipid and so on. It has been reported both experimentally[7] and theoretically[8] that surface tension could induce phase transition.

The challenges to the experimental study of the effects of surface tension on lipid bilayer conformation and function can be attributed to the notorious weak forces involved in lipid bilayers and, consequently, the fragile nature of bilayers. Rutkowski *et al.* studied the mechanical properties of lipid unilamellar vesicles using osmotic-swelling methods[9] but found that large unilamellar vesicles formed from acidic lipids, due to its polydispersity, did not swell in a manner that permitted the computation of a Young's modulus. Hamada *et al.*[7] found that membrane tension could induce phase separation in a homogeneous membrane. They established a quantitative phase diagram of phase organization with respect to applied pressure and temperature for homogeneous membranes. Evans *et al.*[10] have proposed a direct method of tuning the surface tension of a membrane, in which a single giant unilamellar vesicle is held and stretched with a micropipette; they then studied the kinetic process of membrane breakage using a causal sequence of two thermally activated transitions. Atomic force microscopy has also been applied to measure the mechanical properties of a nearly planar freestanding lipid bilayer covering a nanoscopic hole with a defined pore size.[11] The application of this method is, however, limited by the pore size. Recently, Lin *et al.* were able to control the area-per-lipid of a lipid monolayer with a Langmuir trough,[12] but the preparation of a lipid bilayer in a Langmuir trough is not convenient. While great efforts have been made to the experimental study of surface tension's effects on the structure and properties of lipid bilayer, a comprehensive picture is still under construction, to which simulation studies may provide a molecular insight being complementary to the experimental observations.

Growing efforts have been directed to the computational study of properties and behaviors of lipid bilayer membranes.[13] The methods applied to date include self-consistent field theory,[8] dynamical triangulation Monte Carlo,[14] dissipative particle dynamics,[15] all-atom molecular dynamics[16, 17] and coarse grained molecular dynamics[18, 19]. The influences of surface tension on the phase behavior of lipid bilayers are, however, rarely studied.

Cascales *et al*. carried out atomic molecular dynamics simulations of a DPPC bilayer and found that low surface pressures ranging from 0.1 to 1 mN/m did not affect the structure, electrical properties, or hydration of the lipid bilayer. Once the surface pressure was above 40 mN/m, the mesomorphic transition from a liquid crystalline state to a gel state occurred.[20] Uline *et al.* studied the phase behavior of lipid bilayers under different surface tensions using self-consistent field theory[8] and found that an increase in the surface tension decreases the transition temperature from a liquid disordered to a liquid ordered phase in a pure DPPC system. The effect of surface tension on the phase transition of lipid bilayers and its properties, however, has not yet adequately been investigated by such simulations, especially for lipid bilayers embedded with membrane proteins. Our understanding of the effect of surface tension on the structure, function and other properties of lipid bilayers, generated either from experiment or computation, is far from sufficient.

Coarse grained models allows one to study the phase transition of lipid bilayer in a much larger time scale and system size with more generic features. Though the loss in atomic detail information may bring about inaccuracy in describing the dynamics of the process, they could capture the equilibrium properties nicely[21]. The objective of the present study is to obtain insight into the surface tension's effects on the gel/liquid crystal phase transition behavior of lipid bilayers with and without embedded membrane proteins using coarse grained molecular dynamics simulations. While this gel/liquid crystal phase transition may not be directly relevant with biological activities as the liquid-disordered/liquid-ordered transition, the underlying driving forces are highly relevant[21] and these phases may easily induced by adding additional component in the bilayer. What's more, in engineering environments where these biomembranes are used for biosensor or bioseparation, the changes of surface tension and temperature are much larger than in biological environment, the gel/liquid crystal phase change may be more common and more important due to the violent change of bilayer properties between gel and liquid phases. Here a dipalmitoylphosphatidylcholine (DPPC) bilayer, one of the most extensively examined phospholipids in experiments and simulations,[17, 18, 22] was chosen as the model lipid membrane; also, aquaporin (AqpZ), a water channel protein found in a wide range of organisms,[23] was chosen as the embedded membrane protein. Coarse-grained molecular dynamics[24] developed by Marrink *et. al.* were applied to simulate the effects of surface tension on the structure and property of the DPPC bilayer, including area per lipid, lipid order parameters, membrane thickness and planar diffusion coefficients of the lipid molecules. With these we hope to generate insight into the surface tension's effects on the phase transition behavior of lipid bilayers with and without membrane proteins.

Materials and Methods

Model

The simulations were conducted with the Gromacs 4.5.5 platform,[25] using the Martini force field[24, 26] that was first proposed by Marrink *et al.* This coarse grained force field has been well demonstrated to capture the equilibrium properties during the lipid bilayer gel/liquid crystal phase change[21]. Fig. 1(a) and Fig. 1(b) show the coarse-grained model of the pure DPPC bilayer and AqpZ-embedded DPPC bilayer, respectively.

The lipid bilayer was composed of 216 DPPC molecules, which were equally distributed in each layer. We also conducted a series of simulations with a fourth larger pure DPPC bilayer (864 DPPC molecules) at coupling temperature 300K under differing surface tension. The result is the same as for a lipid patch with 216 molecules. This indicates that finite size effect is negligible, which is also observed by R. Faller *et.al* in their simulation of DSPC/DLPC mixtures[18, 27]Each DPPC molecule consists of 12 coarse grained beads with equal 72 amu masses. The *sn*-1 and *sn*-2 acyl tails of a DPPC molecule were represented by four connected hydrophobic apolar beads, C1B to C4B and C1A to C4A, respectively. The polar head group was represented by a negatively charged phosphate group (PO4) and a positively charged choline group (NC3). The glycerol backbone was represented by two neutral beads (GL1 and GL2), among which GL1 linked the phosphate group and the *sn*-2 acyl tail together, while GL2 linked the GL1 and *sn*-1 acyl tail together. The atomic model of AqpZ was obtained from the RCSB Protein Data Bank[23] (PDB code: 1RC2). For the AqpZ-embedded lipid bilayer, the protein was transformed into a coarse grained representation in the Martini force field using a method described elsewhere.[28] The total charge of the protein was zero. To keep the box size in *x*-*y* plane similar, 160 DPPC molecules were arranged around AqpZ. This lipid:protein ratio of 160:1 is typical in biomembrane and in experiments[5]. Four water molecules were treated together as one coarse-grained bead with a mass of 72 amu, denoted as W. The number of solvent particles were 3778 and 3759 for the DPPC bilayer and AqpZ-embedded DPPC bilayer, respectively. A summary for the equilibrium simulations is listed in the ESI Table S1.

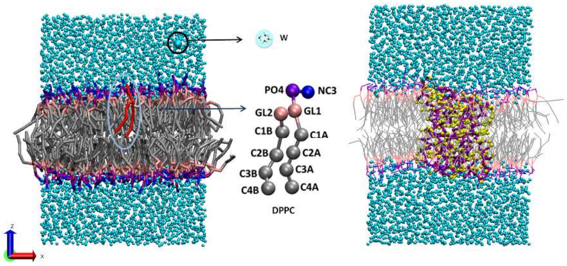

(a) (b)

Fig. 1 DPPC bilayer membrane (a) and DPPC bilayer embedded with AqpZ (b) used in the simulations. The water bead (W) comprises four actual water molecules and is shown in cyan color. AqpZ is shown in Licorice style with the backbone beads colored purple and side chain beads colored yellow. DPPC is consisted of a hydrophilic headgroup (PO4, NC3), intermediate hydrophilic backbone (GL1, GL2), and two acyl tails model by four hydrophobic particles. DPPC is shown in Licorice style (a) and Line style in (b) to clearly show the protein.

Simulation Methods

All the simulations were carried out under periodic boundary conditions. The Berendsen method[29] was used to keep the temperature and pressure constant with coupling constants of 0.2 ps and 0.4 ps, respectively. The temperature coupling was achieved with two groups, each comprised of DPPC molecules (DPPC molecules and protein, for the protein-embedded case) or water beads. The pressure coupling was achieved in a semi-isotropic way with a constant pressure of 1 bar in the direction normal to the membrane (*i.e.* the *z* direction, as shown in Fig. 1) and a constant surface tension in the plane parallel to the membrane plane (*i.e.*, the *x-y* plane, as shown in Fig. 1). According to the standard Martini force field, the electrostatic and Lennard-Jones interactions shifted from 0.0 nm and 0.9 nm to 1.2nm and 1.2 nm, respectively. The integration time step was 40 fs. Considering the advantages of the Martini force field[24] in accelerating the simulation speed, the simulation time shown in this study was four times longer than real time, *i.e.*, 1 μs of simulation time corresponded to 4 μs of real time.

A series of simulated annealing simulations were first conducted to roughly determine the range of temperature and surface tension during which phase transition may occur (ESI†, Fig. S1). Based on these information, equilibrated simulations were designed and conducted. For equilibrated simulations at a given temperature and surface tension, the starting conformation was obtained from the last frame of the 1 μs equilibration runs at 305 K with a zero surface tension. Then, the production runs were run for 8 μs to guarantee the system reached equilibrium. The properties were averaged from the last 2 μs of the simulation trajectories.

Analytical Methods

All properties of the DPPC bilayer at different temperatures and surface tensions were averaged from the last 2 μs of the simulation trajectories, before which the system was equilibrated for at least 6 μs to ensure the system reached equilibrium.

The area per lipid, denoted as APL, which reflects the density of lipid molecules and thickness of the lipid bilayer, was calculated according to the method proposed by Allen *et al.*[30] Briefly, the simulation box was firstly divided into a 20×20 grid in the *x-y* plane. Each grid point was assigned a *z*-value based on the *z* coordinate nearest reference particle (PO4 particle) in the same leaflet. The thickness at that grid point is the difference between the *z*-value in each layer. Points with the same *z*-values correspond to the same reference particle, so the area they occupied was the APL for that reference particle.

The lipid order parameter is defined as

$$S_Z = \frac{3}{2}\langle \cos^2\theta_Z \rangle - \frac{1}{2} \qquad (1)$$

in which θ_z is the angle between the vector defined by two atoms, C3A→C1A, along the positive *z* axis. The value of S_z is between −0.5 and 1. With $S_z = 1$, the C3A→C1A vectors lie parallel or anti-parallel to the *z* direction perfectly, which corresponds to a fully ordered state. While $S_z = 0$ represents a fully disordered state in which the acyl tails move with total freedom.

To obtain the density profile of the DPPC, the box was divided into slices with a thickness of about 0.1 nm in the *z* direction, and the mass densities of the DPPC molecules were calculated in each slice.

Phosphorous group beads (PO4) were used to represent the position of the same molecule when calculating the diffusion coefficients.[31] The lateral diffusion coefficient of the lipids in the membrane plane, *i.e.*, the *x-y* plane, was calculated using the Einstein relation shown in Equation 2, in which $r_i(0)$ is the position of the *i*-th PO4 bead at the initial time ($t_0 = 0$), and $r_i(t)$ is the position of the *i*-th PO4 bead at time t. Only the *x-y* components of the coordinates are considered in the calculation.

$$\lim_{t\to\infty}\left\langle \left\| r_i(t) - r_i(0) \right\|^2 \right\rangle_{i\in A} = 4D_A t \qquad (2)$$

Thermodynamic analysis of surface tension's effects

To probe the effect of surface tension on the phase transition temperature, a thermodynamic relationship was developed[8]. For a pure DPPC bilayer in this work, the internal energy U can be expressed as:

$$U = TS - PV + \gamma A + \mu N \qquad (3)$$

in which T, P, γ, and μ are the temperature, pressure, surface tension, and chemical potential of the lipids, respectively. S, V, A and N are entropy, volume, total area of the lipid layer and total number of lipid molecules, respectively. Thus the Gibbs-Duhem equation is

$$d\mu = -sdT + vdP - ad\gamma \qquad (4)$$

in which s, v, and a are the entropy, volume, and area per lipid, respectively. Equation (4) can be used to describe both the liquid crystal phase and gel phase of the DPPC bilayer, namely

$$d\mu_l = -s_l dT + v_l dP - a_l d\gamma \qquad (5)$$

$$d\mu_g = -s_g dT + v_g dP - a_g d\gamma \qquad (6)$$

where l and g denote the liquid crystal phase and gel phase, respectively.

At the phase transition point, the change of chemical potential should be the same for both phases, *i.e.*, $d\mu_l = d\mu_g$. Thus,

$$-\Delta s dT + \Delta v dP - \Delta a d\gamma = 0 \qquad (7)$$

in which Δs, Δv, Δa represent differences of entropies, volumes and areas per lipid between two phases, respectively.

Here we consider the phase transition of the lipid bilayer as a function of temperature and surface tension, thus based on Equation (7), we have

$$\left(\partial T/\partial\gamma\right)_P = -\Delta a/\Delta s \qquad (8)$$

Since the changes of entropy and areas are both positive when the bilayer changes from gel phase to liquid crystal phase, $(\partial T/\partial\gamma)_p$ is negative.

For the lipid bilayer membrane embedded with membrane protein, the relationship between $(\partial T/\partial\gamma)_p$ and $-\Delta a/\Delta s$ at constant pressure can also be calculated by Equation (8).

Results and discussion

Phase transition under different surface tensions

The change of surface tension and temperature could both induce the phase transition between liquid crystal phase and gel phase for both pure DPPC bilayer and protein embedded DPPC bilayer. The phase transition occurs in several nanoseconds (ESI†, Fig. S1(b)) while lowering the temperature. Properties of the bilayer, like area per lipid, lipid order, bilayer thickness and lipid lateral diffusion coefficients, all show a sharp change near the transition point (Fig. 4~8).

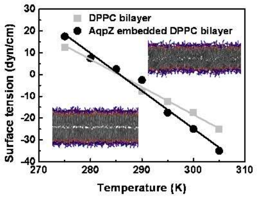

Fig. 2 Relation between critical surface tension and temperature. These data are extracted from the critical point based on the change of APL in Fig.3. Also shown is corresponding snapshot of the pure bilayer. Water beads are not shown for clarity. $(\partial\gamma/\partial T)_p$: DPPC bilayer (−1.27 dyn/(cm·K)), AqpZ-embedded DPPC bilayer (−1.73 dyn/(cm·K)).

Fig. 2 shows the change of the critical surface tension as a function of temperature based on the change of APL as relation of temperature and surface tension in Fig. 3. With a temperature of 285K, the critical surface tension is about 0 dyn/cm, similar as Marrink's results[18] and lower than the experimental value. The coarse grained approximation is responsible for this[19]. As the temperature increases, the critical surface tension decreases linearly, as predicted by the thermodynamic analysis.

For the pure DPPC bilayer, the calculated $(\partial\gamma/\partial T)_p$ is −1.27 dyn/(cm·K), namely, $(\partial T/\partial\gamma)_p$=−0.79 K/(dyn/cm). This agrees well with the value obtained by Uline *et al.* using self-consistent field theory[8] and the experimental results by Portet[32] *et al*. The changes of areas during the phase transition is about 0.13 nm^2, and according to Equation (8), the change of entropies during the phase transition is obtained, *i.e.*, $\Delta s \approx 0.0991 kJ/(K\cdot mol)$, which is similar to the 0.113 $kJ/(K\cdot mol)$ measured by Albon *et. al.*[33]

As for the AqpZ-embedded DPPC bilayer, $(\partial\gamma/\partial T)_p$ is −1.73 dyn/(cm·K), which is smaller than the value for the DPPC bilayer (−1.27 dyn/(cm·K)). This suggests the presence of AqpZ, which is a more rigid building block compared to the lipids, hindered the conformational transition of the lipid bilayer. On the other hand, the (Δs) of the ApqZ-embedded DPPC bilayer is 0.104 kJ/(K·mol), which is similar to the bilayer that does not contain AqpZ. This indicates the AqpZ has a marginal effect on the entropy changes of lipids during phase transitions.

Effects of surface tension on APL

The APL changes of the DPPC bilayer with and without embedded protein were calculated and are shown in Fig. 3. In these cases, 8-μs-long MD simulations at a specific temperature and surface tension were carried out to ensure the systems reached equilibrium. All properties of the DPPC bilayer were obtained from the data collected from the last 2 μs.

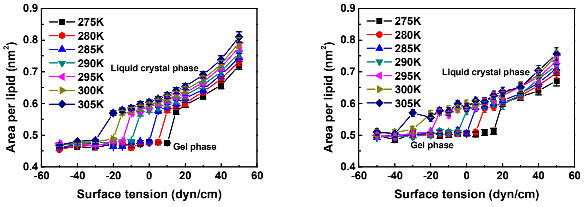

(a) (b)

Fig. 3 Area per lipid (APL) as function of surface tension and temperature for (a) DPPC bilayer; (b) AqpZ-embedded DPPC bilayer at different temperatures. The sharp jumps of the APL denote the phase transition of the bilayer.

It is shown in Fig. 3 that, when the surface tension is 0 dyn/cm, the area per lipid at 305 K is about 0.59 nm^2, which agrees with the value obtained by Marrink *et al.*[24] Once the APL is below 0.47 nm^2, the DPPC bilayer exists in a gel phase.[19] The increase of surface tension from −50 dyn/cm to 50 dyn/cm has little effect on the APL of the gel phase DPPC bilayer. When the APL is above 0.58 nm^2, the DPPC bilayer exists in the liquid crystal phase. Increases in both surface tension and temperature result in significant increases in the APL, *i.e.*, an enhanced fluidity of the lipid bilayer.

Fig. 3(b) shows the changes of the APL of the AqpZ-embedded DPPC bilayer at different temperatures and surface tensions. The critical value of the APL in the gel phase is around 0.5 nm^2, which is slightly higher than that of the pure lipid bilayer (0.47 nm^2), indicating that the presence of AqpZ, which possesses an irregular shape, gives more space for lipid molecules in the bilayer. When the AqpZ-embedded lipid bilayer exists in the gel phase, increasing the surface tension from −50 to 50 dyn/cm has no effect on the APL. When the bilayer is in the liquid crystal phase, although increasing the surface tension leads to an increase in the APL, the enhancement is lower than that of the bilayer without AqpZ, *i.e.*, the interaction between the AqpZ and lipid molecules hindered the fluidity of the DPPC bilayer in the liquid crystal phase.

Effects of surface tension on lipid order

Fig. 4 shows the effect of surface tension on the lipid order parameter (S_z) of the DPPC bilayer at different temperatures.

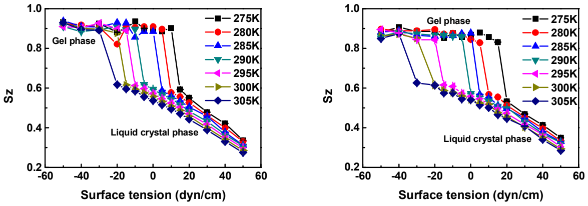

(a) (b)

Fig. 4 Liquid order parameter (S_Z) as a funciton of surface tension for (a) DPPC bilayer; (b) AqpZ-embedded DPPC bilayer at different temperatures.

For the pure DPPC bilayer, as shown in Fig. 4(a), S_z is near 0.9 in the gel phase, indicating that the lipid tails are arranged in nearly parallel order. This is due to the confined movements of the lipids, as shown in Fig. 3(a). It is also shown in Fig. 4(a) that the surface tension has little effect on the value of S_z in the gel phase. For the DPPC in the liquid crystal phase, however, an increase of the surface tension leads to a decrease of S_z from 0.6 to 0.3, *i.e.*, the lipid tails become less ordered.

While a similar response is observed in the AqpZ embedded DPPC bilayer, a major difference is that the value of S_z is lower than that of pure DPPC bilayer in the gel phase. This suggests the presence of AqpZ does not favor the ordered structure of the lipid bilayer in the gel phase. Similar changes have also been shown when carbon nanotube is inserted into the membrane[34, 35]. This may result from the hydrophobic mismatch between the inserted structure and rigid nature of the protein, which renders a non-ideal lipid arrangement, and is similar to the role of cholesterol in tuning the properties of lipid membranes.[36]

The density profile of lipids along the *z* direction

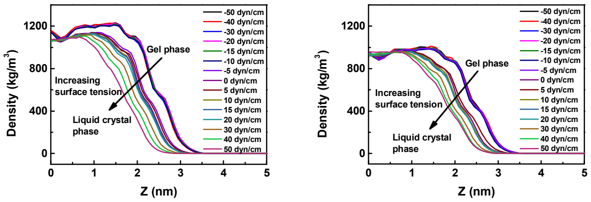

(a) (b)

Fig. 5 Density profile of lipids along the z direction of DPPC bilayer at 290 K for (a) DPPC bilayer; (b) AqpZ-embedded DPPC bilayer. (z = 0 corresponds to the center of the DPPC bilayer membrane).

To illustrate the structure of the lipids in the bilayer, the density profiles of lipid molecules along the *z* direction are calculated and shown in Fig. 5.

Compared to the pure DPPC bilayer shown in Fig. 5(a), the densities of the lipid molecules in the AqpZ-embedded DPPC bilayers are lower at the same surface tensions. This is caused by the volume occupation of AqpZ. It is seen from Fig. 5 that, once in the gel state, a high lateral compaction leads to a higher membrane thickness when AqpZ is present and absent. The density profile remains unchanged under different surface tensions. Once the surface tension exceeds the critical point, the thickness of the lipid bilayer membrane abruptly changes, as shown in Fig. 3 and Fig. 4, *i.e.,* a phase transition occurs. In the case of the liquid crystal phase, the increase in the surface tension leads to a significant decrease in the density of lipids in the bilayer membrane. The response was weakened once AqpZ was embedded into the bilayer, *i.e.*, the interaction with AqpZ enhanced the stability of the lipid bilayer in liquid crystal phase, as shown in Fig. 3 and 4.

Membrane thickness under surface tension

To further display the responses of the DPPC and AqpZ to surface tension, we calculated the thickness of the DPPC bilayer in the *x-y* plane under different surface tensions, the results are given in Fig.6.

Thickness fluctuations were present in all cases, and this reflects the characteristic fluidity of the lipid bilayer. The local thickness of the DPPC bilayer decreases once the surface tension increases, and similar responses were also seen in lipid area 2 nm away from the protein surface in the AqpZ-embedded bilayer. In contrast, the thickness of the lipid bilayer within 2 nm from AqpZ surface showed less significant changes with different surface tension. This results again indicate the stabilization effects of AqpZ.

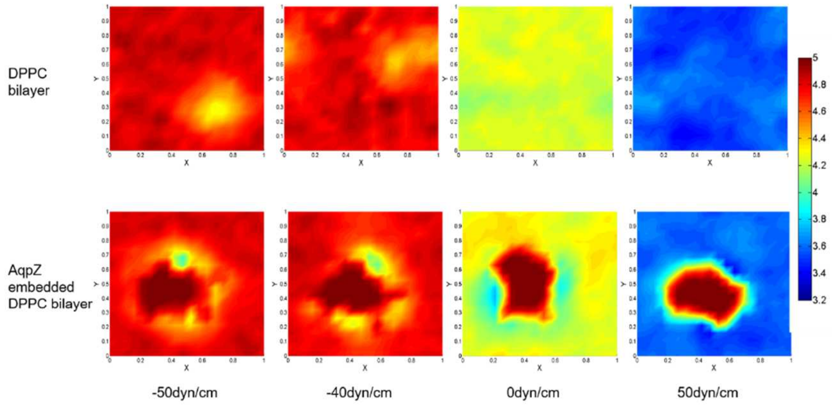

Fig. 6 Bilayer thickness profile in the *x-y* plane for pure DPPC lipid bilayer and AqpZ-embedded DPPC bilayer under different surface tensions at 290 K. The thickness is defined as the distance between a pair of phosphorous group beads in each monolayer at the at the corresponding *x-y* coordinates. Here the *x, y* coordinates has been scaled with the box length.

For AqpZ embedded lipid bilayer with a zero surface tension, we can see that near some part of the protein, the lipid bilayer thickness is lower than the pure DPPC bilayer, about 3.6~4.0nm. This is due to the hydrophobic match between lipid bilayer and protein. All-atom simulations of glyceroporin GlpF[37], another typical member of the aquaporin family, in POPC or POPE bilayer found similar behavior with a bilayer thickness of about 3.6nm near GlpF. We can also see that the bilayer thickness near the protein surface is not the same and the fluctuation is about 1nm. Since we used AqpZ monomer, this could be the reason for why AqpZ monomer could function independently but usually exist in the form of tetramer[38] in biological environment.

For cases with surface tension lower than zero, the bilayer thickness near the protein are larger than 3.6nm, but still lower than that of the corresponding pure DPPC bilayer. Whereas for lipid bilayer with high surface tension, the lipid bilayer thickness near the protein is larger than that of the pure lipid bilayer. These above discussions show that surface tension is an important factor to tune the hydrophobic match/mismatch between lipid bilayer and membrane protein, thus controlling the structure and functions of the protein.

Lateral movement of DPPC molecules in the bilayer

The movement of lipid molecules can be clarified into two categories, translocation of lipid molecules in the parallel direction of the membrane and flipping of lipid molecules between two monolayers of the membrane. For the present study, the simulation time was not sufficient to display the flipping of lipid molecules. Here we monitored the translocation of lipids in the parallel direction in the *x-y* plane, and then calculated the diffusion coefficient using the method described above. The results are given in Fig. 7.

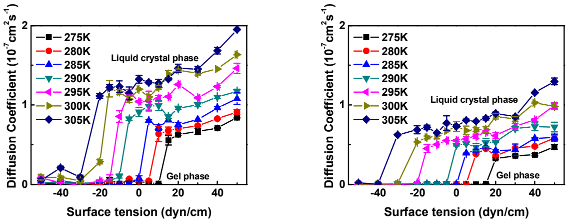

Fig. 7 Lateral diffusion coefficients of DPPC molecules in lipid bilayers for (a) DPPC bilayer; (b) AqpZ-embedded DPPC bilayer.

As shown in Fig. 7, the average diffusion coefficients in the gel phase for both the pure DPPC bilayer and the AqpZ-embedded bilayer are around $\sim 1\times 10^{-9}\text{cm}^2\cdot\text{s}^{-1}$; this value is one or two orders of magnitude lower than that in the liquid crystal phase. In all cases, the increase in either temperature or surface tension increases the fluidity of the lipid bilayer. The presence of the membrane protein in the lipid bilayer when in the liquid crystal phase hindered the fluidity of the lipid bilayer. This is similar to cholesterol in tuning the properties of lipid membranes.[36]

Conclusions

The present study has probed, by coarse-grained molecular dynamics simulation, the effects of surface tensions on the structural transition of a DPPC lipid bilayer. In the gel phase when the ordered lipid molecules are densely compacted, the surface tension has a marginal effect on the structure as indexed by the area per lipid, the lipid order parameter, the density profile and the thickness of the DPPC bilayer; this was also the case for the lateral movement of the lipid molecules, as indexed by the lateral diffusion coefficients of lipid molecules. Once in the liquid crystal phase, the increase in the surface tension increases the APL and the lateral diffusion coefficients of lipid molecules while it decreases the lipid order parameter and the thickness of the lipid bilayer, *i.e.*, the fluidity of the bilayer increases. The addition of the membrane protein (AqpZ) makes the bilayer less sensitive to the surface tension. For the lipid bilayer in the gel phase, the presence of the membrane protein led to a less ordered structure compared to the pure lipid bilayer. For the lipid bilayer in the lipid crystal phase, the membrane protein hindered the parallel movements of lipid molecules and thus reduced the fluidity of the lipid bilayer. The above simulation established some insight into the phase transition of the lipid bilayer as a function of surface tension, which is helpful for understanding and utilizing lipid bilayers.

Acknowledgements

The authors are grateful to the Chinese National Natural Science Foundation for financial support of this project (No. 21276138) and 973 Project (No.2013CB733604).

Notes and references

[a] *Department of Chemical Engineering, Tsinghua University, Beijing, 100084, China. E-mail: *ludiannan@tsinghua.edu.cn; liuzheng@mail.tsinghua.edu.cn.*

[b] *Key Laboratory of Bioorganic Phosphorous Chemistry and Chemical Biology (Ministry of Education), Department of Chemistry, Tsinghua University, Beijing 100084, P. R. China.*

† Electronic Supplementary Information (ESI) available. See DOI: 10.1039/b000000x/

References

1. T. J. McIntosh and S. A. Simon, *Annu Rev Bioph Biom*, 2006, 35, 177-198.
2. R. C. Hardie and K. Franze, *Science*, 2012, 338, 260-263.
3. N. Wang, J. P. Butler and D. E. Ingber, *Science*, 1993, 260, 1124-1127.
4. C. H. Nielsen, *Anal Bioanal Chem*, 2009, 395, 697-718.
5. Y. Zhao, A. Vararattanavech, X. S. Li, C. HelixNielsen, T. Vissing, J. Torres, R. Wang, A. G. Fane and C. Y. Tang, *Environ Sci Technol*, 2013, 47, 1496-1503.
6. G. Soveral, R. I. Macey and T. F. Moura, *Biol Cell*, 1997, 89, 275-282.
7. T. Hamada, Y. Kishimoto, T. Nagasaki and M. Takagi, *Soft Matter*, 2011, 7, 9061-9068.
8. M. J. Uline, M. Schick and I. Szleifer, *Biophys J*, 2012, 102, 517-522.
9. C. A. Rutkowski, L. M. Williams, T. H. Haines and H. Z. Cummins, *Biochemistry-Us*, 1991, 30, 5688-5696.
10. E. Evans, V. Heinrich, F. Ludwig and W. Rawicz, *Biophys J*, 2003, 85, 2342-2350.
11. S. Steltenkamp, M. M. Muller, M. Deserno, C. Hennesthal, C. Steinem and A. Janshoff, *Biophys J*, 2006, 91, 217-226.
12. B. Lin, M. C. Shih, T. M. Bohanon, G. E. Ice and P. Dutta, *Phys Rev Lett*, 1990, 65, 191-194.
13. L. Bagatolli and P. B. S. Kumar, *Soft Matter*, 2009, 5, 3234-3248.
14. P. B. S. Kumar and M. Rao, *Mol Cryst Liq Crys A*, 1996, 288, 105-118.
15. S. Yamamoto and S. Hyodo, *J Chem Phys*, 2003, 118, 7937-7943.
16. S. S. Qin, Z. W. Yu and Y. X. Yu, *J Phys Chem B*, 2009, 113, 8114-8123.
17. S. Leekumjorn and A. K. Sum, *Bba-Biomembranes*, 2007, 1768, 354-365.
18. S. J. Marrink, J. Risselada and A. E. Mark, *Chem Phys Lipids*, 2005, 135, 223-244.
19. K. Lai, B. A. Wang, Y. Zhang and Y. W. Zhang, *Phys Chem Chem Phys*, 2012, 14, 5744-5752.
20. J. J. L. Cascales, T. F. Otero, A. J. F. Romero and L. Camacho, *Langmuir*, 2006, 22, 5818-5824.
21. J. M. Rodgers, J. Sorensen, F. J. M. de Meyer, B. Schiott and B. Smit, *J Phys Chem B*, 2012, 116, 1551-1569.
22. Z. V. Leonenko, E. Finot, H. Ma, T. E. S. Dahms and D. T. Cramb, *Biophys J*, 2004, 86, 3783-3793.
23. D. F. Savage, P. F. Egea, Y. Robles-Colmenares, J. D. O'Connell and R. M. Stroud, *Plos Biol*, 2003, 1, 334-340.
24. S. J. Marrink, A. H. de Vries and A. E. Mark, *J Phys Chem B*, 2004, 108, 750-760.
25. S. Pronk, S. Pall, R. Schulz, P. Larsson, P. Bjelkmar, R. Apostolov, M. R. Shirts, J. C. Smith, P. M. Kasson, D. van der Spoel, B. Hess and E. Lindahl, *Bioinformatics*, 2013, 29, 845-854.
26. S. J. Marrink, H. J. Risselada, S. Yefimov, D. P. Tieleman and A. H. de Vries, *J Phys Chem B*, 2007, 111, 7812-7824.

27. R. Faller and S. J. Marrink, *Langmuir*, 2004, 20, 7686-7693.
28. L. Monticelli, S. K. Kandasamy, X. Periole, R. G. Larson, D. P. Tieleman and S. J. Marrink, *J Chem Theory Comput*, 2008, 4, 819-834.
29. H. J. C. Berendsen, J. P. M. Postma, W. F. Vangunsteren, A. Dinola and J. R. Haak, *J Chem Phys*, 1984, 81, 3684-3690.
30. W. J. Allen, J. A. Lemkul and D. R. Bevan, *J Comput Chem*, 2009, 30, 1952-1958.
31. M. P. Allen, Tildesley, D. J., *Computer Simulations of Liquids*, Oxford: Oxford Science Publications, 1987.
32. T. Portet, S. E. Gordon and S. L. Keller, *Biophys J*, 2012, 103, L35-L37.
33. N. Albon and J. M. Sturtevant, *Proc Natl Acad Sci U S A*, 1978, 75, 2258-2260.
34. S. O. Nielsen, B. Ensing, V. Ortiz, P. B. Moore and M. L. Klein, *Biophys J*, 2005, 88, 3822-3828.
35. B. Liu, X. Y. Li, B. L. Li, B. Q. Xu and Y. L. Zhao, *Nano Lett*, 2009, 9, 1386-1394.
36. R. A. Cooper, *J Supramol Str Cell*, 1978, 8, 413-430.
37. M. O. Jensen and O. G. Mouritsen, *Bba-Biomembranes*, 2004, 1666, 205-226.
38. J. B. Heymann and A. Engel, *News Physiol Sci*, 1999, 14, 187-193.